Western University
Scholarship@Western

Medical Biophysics Publications | Medical Biophysics Department

7-1-2010

Chronic obstructive pulmonary disease: Longitudinal hyperpolarized (3)He MR imaging

Miranda Kirby

Lindsay Mathew

Andrew Wheatley

Giles E Santyr

David G McCormack

See next page for additional authors

Follow this and additional works at: https://ir.lib.uwo.ca/biophysicspub

 Part of the Medical Biophysics Commons

Citation of this paper:
Kirby, Miranda; Mathew, Lindsay; Wheatley, Andrew; Santyr, Giles E; McCormack, David G; and Parraga, Grace, "Chronic obstructive pulmonary disease: Longitudinal hyperpolarized (3)He MR imaging" (2010). *Medical Biophysics Publications*. 146.
https://ir.lib.uwo.ca/biophysicspub/146

Authors
Miranda Kirby, Lindsay Mathew, Andrew Wheatley, Giles E Santyr, David G McCormack, and Grace Parraga

This article is available at Scholarship@Western: https://ir.lib.uwo.ca/biophysicspub/146

Note: This copy is for your personal, non-commercial use only. To order presentation-ready copies for distribution to your colleagues or clients, contact us at www.rsna.org/rsnarights.

Chronic Obstructive Pulmonary Disease: Longitudinal Hyperpolarized ^{3}He MR Imaging[1]

Miranda Kirby, BSc
Lindsay Mathew, BMSc
Andrew Wheatley, BSc
Giles E. Santyr, PhD
David G. McCormack, MD
Grace Parraga, PhD

Purpose: To quantitatively evaluate a small pilot group of ex-smokers with chronic obstructive pulmonary disease (COPD) and healthy volunteers during approximately 2 years by using hyperpolarized helium 3 (^{3}He) magnetic resonance (MR) imaging.

Materials and Methods: All subjects provided written informed consent to the study protocol, which was approved by the local research ethics board and Health Canada and was compliant with the Personal Information Protection and Electronic Documents Act and HIPAA. Hyperpolarized ^{3}He MR imaging, hydrogen 1 MR imaging, spirometry, and plethysmography were performed in 15 ex-smokers with COPD and five healthy volunteers (with the same mean age and age range) at baseline and 26 months ± 2 (standard deviation) later. Apparent diffusion coefficients (ADCs) derived from ^{3}He MR imaging were calculated from diffusion-weighted ^{3}He MR images, and ^{3}He ventilation defect volume (VDV) and ventilation defect percentage (VDP) were generated after manual segmentation of ^{3}He MR spin-density images.

Results: For subjects with COPD, significant increases in ^{3}He MR imaging–derived VDV (P = .03), VDP (P = .006), and ADC (P = .02) were detected, whereas there was no significant change in forced expiratory volume in 1 second (FEV_1) (P = .97). For healthy never-smokers, there was no significant change in imaging or pulmonary function measurements at follow-up. There was a significant correlation between changes in FEV_1 and changes in VDV (r = −0.70, P = .02) and VDP (r = −0.70, P = .03).

Conclusion: For this small pilot group of ex-smokers with COPD, ^{3}He MR imaging–derived VDV, VDP, and ADC measurements worsened significantly, but there was no significant change in FEV_1, suggesting increased sensitivity of hyperpolarized ^{3}He MR imaging for depicting COPD changes during short time periods.

©RSNA, 2010

Supplemental material: *http://radiology.rsna.org/lookup/suppl/doi:10.1148/radiol.10091937/-/DC1*

[1] From the Imaging Research Laboratories, Robarts Research Institute, 100 Perth Dr, PO Box 5015, London, ON, Canada N6A 5K8 (M.K., L.M., A.W., G.E.S., G.P.); and Department of Medical Biophysics (M.K., L.M., G.E.S., G.P.) and Division of Respirology, Department of Medicine (D.G.M.), the University of Western Ontario, London, Ontario, Canada. Received October 16, 2009; revision requested December 15; revision received December 23; accepted January 6, 2010; final version accepted January 13. Supported by the Ontario Research Fund, Canadian Institutes of Health Research, and Academic Medical Organization of Southwestern Ontario. M.K. and L.M. supported by the Schulich Graduate Research Fund, provided by the University of Western Ontario, and fellowship awards from the Canadian Institutes of Health Research Strategic Training Program. **Address correspondence to** G.P. (e-mail: *gep@imaging.robarts.ca*).

©RSNA, 2010

Chronic obstructive pulmonary disease (COPD) is a leading cause of morbidity and mortality and affects at least 600 million people worldwide (1). It is the world's fourth leading cause of death and the most common chronic, terminal respiratory disease (2). Because of the heterogeneous nature of COPD, studies of its natural history and progression are complex, typically requiring large-study sample sizes and long durations to obtain relevant longitudinal end points. Accordingly, much of our current understanding of the natural history of COPD arises from the landmark study of Fletcher and Peto (3) and is based on cross-sectional spirometric measurements of forced expiratory volume in 1 second (FEV_1). The current functional definition of COPD (4) is also based on FEV_1, and change in FEV_1 over the course of time is still the most widely accepted measure of COPD progression. However, a number of limitations of spirometry for the diagnosis, classification, and longitudinal monitoring of COPD are motivating the development of new COPD measurements (5), including those derived from noninvasive imaging (6,7). For example, thin-section multidetector computed tomography (CT) (8–11) has been used to identify phenotypes of both emphysema and airway disease (12–14) and depicts significant COPD changes during relatively short periods of time (15).

Hyperpolarized helium 3 (^{3}He) magnetic resonance (MR) imaging has recently emerged as another research method for the evaluation of COPD (16–20). In particular, previous work showed that the apparent diffusion coefficient (ADC) derived from ^{3}He MR imaging (16,21–23) was a sensitive measurement of emphysematous destruction (19,23,24) and airspace size (16,17,25,26) and correlated with pulmonary function (FEV_1 and diffusing capacity of lung for carbon monoxide) (27), as well as histologic measurements of lung surface area (28). Importantly, ^{3}He MR imaging–derived ADC is also age dependent (29) and reflects differences in patient anatomic position (30), disease severity (31), and smoking history (32). Quantitative focal ^{3}He MR imaging–derived ventilation defects have also been shown in COPD (24,32–34), and these reflect differences in subject age (35) and disease status (20). To better understand the potential for hyperpolarized ^{3}He MR imaging to provide quantitative longitudinal COPD end points, we designed a pilot longitudinal ^{3}He MR imaging study of COPD. The purpose of this study was to quantitatively evaluate a small pilot group of ex-smokers with COPD and healthy volunteers over the course of approximately 2 years by using hyperpolarized ^{3}He MR imaging.

Advances in Knowledge

- In a small group of ex-smokers with chronic obstructive pulmonary disease (COPD), hyperpolarized ^{3}He MR imaging measurements showed significant progression after 26 months, whereas forced expiratory volume in 1 second (FEV_1) did not significantly change.
- There was a significant inverse correlation between changes in ^{3}He MR imaging–derived ventilation defect volume measurements and FEV_1.
- Hyperpolarized ^{3}He MR imaging is a sensitive tool for the quantitative longitudinal evaluation of COPD.

Implication for Patient Care

- In a small group of ex-smokers with COPD, hyperpolarized ^{3}He MR imaging depicted significant changes in apparent diffusion coefficient and ventilation measurements, whereas there was no significant change in FEV_1; this finding suggests that regional ^{3}He MR imaging measurements provide adequate sensitivity for detecting COPD changes during relatively short time periods, before significant changes in FEV_1 can be detected.

Materials and Methods

Subjects

Twenty subjects were enrolled from the general population of the local tertiary health care center, as previously described (20). All subjects provided written informed consent to the study protocol, which was approved by the local research ethics board and Health Canada, and the study was compliant with the Personal Information Protection and Electronic Documents Act and the Health Insurance Portability and Accountability Act. Subjects with COPD were enrolled who were ex-smokers between the ages of 50–70 years and who had a clinical diagnosis of COPD. Those enrolled subjects with COPD were categorized according to the Global Initiative for Chronic Obstructive Lung Disease criteria (4) and had a smoking history of at least 10 pack-years and had fewer than three COPD exacerbations within the past 12 months. Exacerbations during the follow-up period were defined as hospitalization for COPD or as the patient's first-time need for antibiotic or prednisone therapy, and these were reported from hospital records (36) and subject charts and were additionally verified with a telephone interview with the subject after follow-up imaging was completed. Subjects with COPD were excluded during a screening visit

Published online
10.1148/radiol.10091937

Radiology 2010; 256:280–289

Abbreviations:
ADC = apparent diffusion coefficient
COPD = chronic obstructive pulmonary disease
FEV_1 = forced expiratory volume in 1 second
VDV = ventilation defect volume
VDP = ventilation defect percentage

Author contributions:
Guarantor of integrity of entire study, G.P.; study concepts/study design or data acquisition or data analysis/interpretation, all authors; manuscript drafting or manuscript revision for important intellectual content, all authors; manuscript final version approval, all authors; literature research, M.K., L.M., G.P.; clinical studies, M.K., A.W., D.G.M., G.P.; statistical analysis, M.K., A.W., G.P.; and manuscript editing, M.K., L.M., A.W., D.G.M., G.P.

Authors stated no financial relationship to disclose.

if FEV_1 was greater than 3% after administration of salbutamol. Healthy volunteers were enrolled (same age range as the subjects with COPD) who had a smoking history of less than 1 pack-year with no smoking in the previous 25 years and no history of previous chronic or current respiratory disease. All tests and imaging were performed at baseline and at 26 months ± 2 (standard deviation).

Pulmonary Function Tests

Spirometry was performed by using a spirometer (ndd EasyOne; Medizintechnik, Zurich, Switzerland) to report FEV_1 and forced vital capacity with a minimum of three acceptable spirometry maneuvers; the best FEV_1 and forced vital capacity were selected for analysis according to American Thoracic Society guidelines (37). Whole-body plethysmography was performed by using a stand-alone body plethysmograph (Elite Series; MedGraphics, St Paul, Minn) for the measurement of total lung capacity, inspiratory capacity, residual volume, and functional residual capacity.

MR Imaging

Subjects were screened for MR imaging and coil compatibility (inner diameter of elliptical coil = 50 cm) prior to imaging, and digital pulse oximetry was used to monitor arterial blood oxygenation levels during breath-hold MR imaging. A turnkey, spin-exchange polarizer system (HeliSpin; GE Healthcare, Durham, NC) was used to polarize ^{3}He gas to 30%–40%, as previously described (38). Doses of hyperpolarized ^{3}He gas (5 mL per kilogram of body weight) were administered in 1-L plastic bags (Tedlar; Jensen Inert Products, Coral Springs, Fla) and were diluted with ultrahigh purity, medical-grade nitrogen (Spectra Gases, Alpha, NJ). Polarization of the diluted dose was quantified at a polarimetry station (GE Healthcare, Durham, NC) immediately prior to ^{3}He gas administration to subject.

MR imaging was performed with a whole-body 3.0-T MR imaging system (Excite 12.0; GE Healthcare, Milwaukee, Wis) with broadband imaging capability, as previously described (33). All ^{3}He MR imaging was performed with a whole-body gradient set with a maximum gradient amplitude of 1.94 G/cm and a single-channel, rigid elliptical transmit-receive chest coil (RAPID Biomedical, Würzburg, Germany). The basis frequency of the coil was 97.3 MHz, and excitation power was 3.2 kW by using a radiofrequency power amplifier (AMT 3T90; GE Healthcare, Milwaukee, Wis).

Coronal two-dimensional multiple-section hydrogen 1 (^{1}H) images were acquired prior to ^{3}He MR imaging, with subjects imaged during 1-L breath hold of the ^{4}He-N_2 mixture from a starting point of functional residual capacity by using a whole-body radiofrequency coil and a proton fast spoiled-gradient-echo sequence (16-second total data acquisition; repetition time msec/echo time msec, 4.7/1.2; flip angle, 30°; field of view, 40 × 40 cm; matrix, 256 × 256; 14 sections; 15-mm section thickness; 0-cm intersection gap). For diffusion-weighted imaging, coronal multisection images were obtained by using a fast gradient-echo method with centric k-space sampling. Two interleaved images (14-second total data acquisition; 7.6/3.7; flip angle, 8°; field of view, 40 × 40 cm; matrix, 128 × 128; seven sections; 30-mm section thickness), with and without additional diffusion sensitization (maximum gradient amplitude = 1.94 G/cm, rise and fall time = 0.5 msec, gradient duration = 0.46 msec, diffusion time = 1.46 msec, *b* value = 1.6 sec/cm^2), were acquired. For ventilation, or spin-density, imaging, coronal multisection images were obtained by using the same ^{3}He coil (14-second total data acquisition; 4.3/1.4; flip angle, 7°; bandwidth, 31.25 kHz; field of view, 40 × 40 cm; matrix, 128 × 128; 14 sections; 15-mm section thickness; 0-cm intersection gap) and multisection two-dimensional simultaneous acquisition of a ventilation image (no T1-weighted sensitization) and a T1-weighted image. Only images without T1-weighting were used for ventilation analysis in this study. All imaging was completed within approximately 7–10 minutes of subjects first lying in the imager.

Image Analysis

The signal-to-noise ratio for all images acquired was determined by calculating the mean pixel value within a 10 × 10-voxel region of interest for four representative regions of interest within the lung parenchyma and dividing by the standard deviation of the mean pixel values for noise inside a region of interest of the same size at the corners of the image where there was no lung structure. Signal-to-noise ratio was determined for each section and then was averaged to obtain a single signal-to-noise ratio for each subject and time point. Images were analyzed in a controlled image visualization environment with room lighting levels equivalently established for all image analysis sessions.

ADC maps were processed by using in-house software programmed in the interactive data language Virtual Machine platform (Research Systems, Denver, Colo) as previously described (33) with a *b* value of 1.6 sec/cm^2. Spin-density images were examined for analysis of ventilation defects in all coronal sections by two expert observers (M.K. and L.M.) blinded to subject identity, disease status, and time point, as well as the other observer's measurements. As previously described (39), a ventilation defect was identified by each observer independently as any lung region of diminished signal intensity but not those areas of signal loss associated with the pulmonary vascular structures, heart, hilum, and mediastinum. Images were reviewed such that ^{3}He and ^{1}H images were visible on a digital workstation monitor system (consisting of identical 19-inch flat panel monitors). Manual segmentation of ventilation defects was performed by using custom-designed image visualization software that also provided a method for two-dimensional rigid single-point image registration (^{1}H and ^{3}He sections) based on the carina, which facilitated the manual segmentation of ventilation defects in all sections. Ventilation defect volume (VDV) and thoracic cavity volume were recorded following manual segmentation of ^{3}He and ^{1}H images, respectively, and were used to calculate ventilation defect percentage (VDP) (16,25,26,40). VDV was derived from the manually

Table 1

Subject Demographic Characteristics in Ex-Smokers with COPD and Never-Smokers

	Healthy Never-Smokers (n = 5)		Ex-Smokers with COPD (n = 15)	
Parameter	Baseline	Follow-up	Baseline	Follow-up
Age (y)	69 ± 6 (58–74)	72 ± 6 (61–76)	68 ± 6 (59–75)	70 ± 5 (61–77)
No. of men	2	2	8	8
Body mass index (kg/m^2)	25 ± 2 (24–29)	25 ± 2 (23–28)	28 ± 5 (19–38)	27 ± 5 (18–37)
FEV_1 (L)	2.77 ± 1.01	2.62 ± 0.93	1.51 ± 0.63	1.43 ± 0.56
FEV_1 (percentage predicted)	110 ± 23	107 ± 23	53 ± 15	52 ± 15
FEV_1/FVC ratio	77 ± 4	78 ± 15	45 ± 14	49 ± 16
Inspiratory capacity (%)	106 ± 18	...	88 ± 23	82 ± 22
Reserve volume (%)	95 ± 15	...	157 ± 48	132 ± 33
Functional residual capacity (%)	101 ± 12	...	145 ± 65	131 ± 33
Total lung capacity (%)	105 ± 12	...	109 ± 17	105 ± 10

Note.—Unless otherwise indicated, data are means ± standard deviations, with ranges in parentheses.

segmented ventilation defect area for each section, and this was multiplied by the section thickness; VDV for all sections was summed to obtain whole-lung VDV. For the center section, which was the middle section acquired that clearly showed the carina and two main bronchi, VDV was also manually segmented and reported. In addition, whole-lung and center-section measurements were recorded for thoracic cavity volume for calculation of whole-lung and center-section VDP, as well as for ADC.

Statistical Methods

For ^{3}He MR imaging ventilation measurements, observer reproducibility was evaluated for two observers by using the interclass correlation coefficient, coefficient of variation, and linear regression (r^2) by using software (SPSS, version 16.00; SPSS, Chicago, Ill). Comparison of baseline and follow-up means was performed by using a Wilcoxon matched-pairs two-tailed t test (SPSS, version 16.00). The relationship between changes in ^{3}He MR imaging measurements and changes in pulmonary function measurements at follow-up was determined by using linear regression and Spearman correlation coefficients by using software (Prism, version 4.00; GraphPad Software, San Diego, Calif). The relationship between the changes in ^{3}He MR imaging–derived VDV and smoking history was determined by using linear regression and Spearman correlation coefficients (Prism, version 4.00). The Holm-Bonferroni correction (41) was used for multiple paired t tests and all correlations. The Holm-Bonferroni–adjusted P values were determined by ordering P values from smallest to largest, with the smallest P value multiplied by k, where k is the number of hypotheses to be tested. If the resulting modified P value was less than α (type I error rate), the hypothesis was rejected. The next smallest P value was then multiplied by $k - 1$, and the new modified P value was compared with α. This process was repeated until the modified P value could not be rejected. In all statistical analyses, results were considered significant when the probability of making a type I error was less than 5% ($P < .05$). A retrospective sample size (n) calculation was performed to detect a significant change (δ) in FEV_1 with α equal to .05 and power β equal to .80 and where SD is standard deviation; accordingly, Z_α was 1.96 and Z_β was 0.2, and n was calculated according to the following equation (42):

$$n = \frac{2\left(Z_\alpha + Z_\beta\right)^2 \mathrm{SD}^2}{\delta^2}.$$

Results

Demographic characteristics are provided in Table 1. All subjects with COPD were nonsmokers at baseline with a mean smoking history of 47 pack-years ± 22 (range, 11–85 pack-years) and mean years of not smoking at baseline of 11 years ± 10 (range, 10 weeks to 34 years). Three subjects experienced a single COPD exacerbation during the follow-up period.

Table 2 shows mean and median whole-lung and center-section hyperpolarized ^{3}He MR imaging measurements for healthy never-smokers and subjects with COPD. The absolute change and annualized rates of change of FEV_1 and hyperpolarized ^{3}He MR imaging measurements for subjects with COPD are provided in Table 3. For ADC, annualized rate of change for ex-smokers with COPD was 0.01 cm^2/sec and that for never-smokers was 0.002 cm^2/sec. There was no significant association between the changes in image signal-to-noise ratio and the changes in ADC ($r = -0.51$, $P = .12$) and VDV ($r = -0.17$, $P = .55$). Interobserver reproducibility of ^{3}He MR imaging–derived VDV was previously evaluated for three observers, and this was the same as intraobserver variability (coefficient of variation = 10%, unpublished results). For two observers, interobserver reproducibility was assessed for whole-lung VDV (interclass correlation coefficient = 0.93, coefficient of variation = 38%, and $r^2 = 0.84$ [$P < .0001$]) and whole-lung VDP (interclass correlation coefficient = 0.91, coefficient of variation = 43%, and $r^2 = 0.81$ [$P < .0001$]).

Table 2

Helium 3 MR Imaging–derived ADC and Ventilation Defect Measurements at Baseline and Follow-up

	Healthy Never-Smokers (n = 5)		Ex-Smokers with COPD (n = 15)	
Parameter	Baseline	Follow-up	Baseline	Follow-up
Whole-lung ADC (cm^2/sec)	0.27 (0.25) [0.02]	0.29 (0.29) [0.03]	0.43 (0.45) [0.08]	0.46 (0.46) [0.07]
Center-section ADC (cm^2/sec)	0.28 (0.27) [0.02]	0.28 (0.30) [0.03]	0.44 (0.45) [0.09]	0.47 (0.46) [0.08]
Whole-lung VDV (L)	0.023 (0.006) [0.04]	0.020 (0.017) [0.02]	0.52 (0.24) [0.54]	0.92 (0.77) [0.93]
Center-section VDV (L)	0.003 (0.000) [0.005]	0.002 (0.001) [0.002]	0.056 (0.023) [0.053]	0.11 (0.11) [0.11]
Whole-lung VDP (%)	0.5 (0.2) [0.9]	0.5 (0.5) [0.4]	9 (6) [9]	16 (15) [14]
Center-section VDP (%)	0.6 (0.2) [0.9]	0.4 (0.2) [0.4]	9 (11) [13]	16 (16) [22]

Note.—Data are means, with medians in parentheses and standard deviations in brackets.

Figure E1 (online) shows the relationship between ventilation defect measurements (whole-lung VDV [r^2 = 0.84, $P <$ .0001] and whole-lung VDP [r^2 = 0.81, $P <$ .0001]) for observer 1 and 2. The change at follow-up for observer 1 and 2 were significantly correlated for whole-lung VDV (r^2 = 0.51, P = .0004) and whole-lung VDP (r^2 = 0.39, P = .007). The change in whole-lung VDV and whole-lung VDP for each observer and the mean for both observers is provided in Table E1 (online), and throughout the main body of the article, a single observer's results are described. Table E2 (online) shows a subject listing of baseline and follow-up pulmonary function and ^{3}He MR imaging measurements.

Wilcoxon matched-pairs two-tailed t tests indicated that all ^{3}He MR imaging measurements were significantly different at follow-up for subjects with COPD. There was no significant change observed in FEV_1 (percentage predicted) for subjects with COPD at follow-up. For healthy never-smokers, there was no detectable change in any pulmonary function or imaging measurement. The changes detected in the ex-smokers with COPD were significantly different than the changes measured in the healthy volunteers for whole-lung VDV (P = .04) and whole-lung VDP (P = .01) but were not significantly different for whole-lung ADC (P = .96) or FEV_1 (P = .21).

Figure 1 shows ventilation images, ADC maps, and ADC histograms for two representative healthy never-smokers at baseline and follow-up. Figure 2 shows ventilation images, ADC maps, and ADC histograms for two representative

Table 3

Annualized Change in Pulmonary Function and ^{3}He MR Imaging Measurements in Subjects with COPD at Follow-up

Parameter	Absolute Change	Annualized Rate of Change	P Value*
FEV_1 (percentage predicted)	−1	−0.4	.97 (.97)
Whole-lung ADC (cm^2/sec)	0.02	0.01	.01 (.02)
Center-section ADC (cm^2/sec)	0.03	0.01	.004 (.02)
Whole-lung VDV (L)	0.4	0.20	.007 (.03)
Center-section VDV (L)	0.05	0.03	.003 (.02)
Whole-lung VDP (%)	7	4	.0009 (.006)
Center-section VDP (%)	7	3	.01 (.03)

* Data are P values determined with Wilcoxon matched-pairs two-tailed t tests, with Holm-Bonferroni–adjusted P values in parentheses.

subjects with COPD at baseline and follow-up.

Table 4 shows Spearman correlation coefficients for the relationship between the changes in FEV_1 (absolute and percentage predicted) and those in ^{3}He MR imaging–derived ADC, VDV, and VDP for subjects with COPD. As shown in Figure 3, the change in FEV_1 (absolute) showed a significant negative association with the change in center-section VDV (r = −0.70, P = .02) and center-section VDP (r = −0.70, P = .03) but not with the change in ADC. Thoracic cavity volume was calculated for all subjects from ^{1}H MR imaging of the thoracic cavity, and for all subjects, the change in thoracic cavity volume was significantly correlated with the change in total lung capacity measured by using plethysmography (r = 0.81, P = .001). Figure 4 shows the relationships between smoking history of patients with COPD (pack-years smoking) and the changes in ^{3}He MR imaging–derived VDV and FEV_1. There was no significant correlation between pack-years smoking and the change in FEV_1 (r = 0.05, P = .83), and the relationship between pack-years smoking and whole-lung VDV was moderate, but once corrected for multiple tests, this relationship was on the threshold of significance (whole-lung VDV [r = 0.52; P = .02, uncorrected; P = .06, Holm-Bonferroni corrected]).

Discussion

Several observations were made in this small longitudinal pilot study. First, we observed that mean ^{3}He MR imaging–derived ADC, VDV, and VDP significantly increased during the 26-month follow-up period in 15 ex-smokers with COPD, whereas pulmonary function measurements did not significantly change during the same time period. Because of the previously reported and pioneering epidemiologic findings of

Figure 1

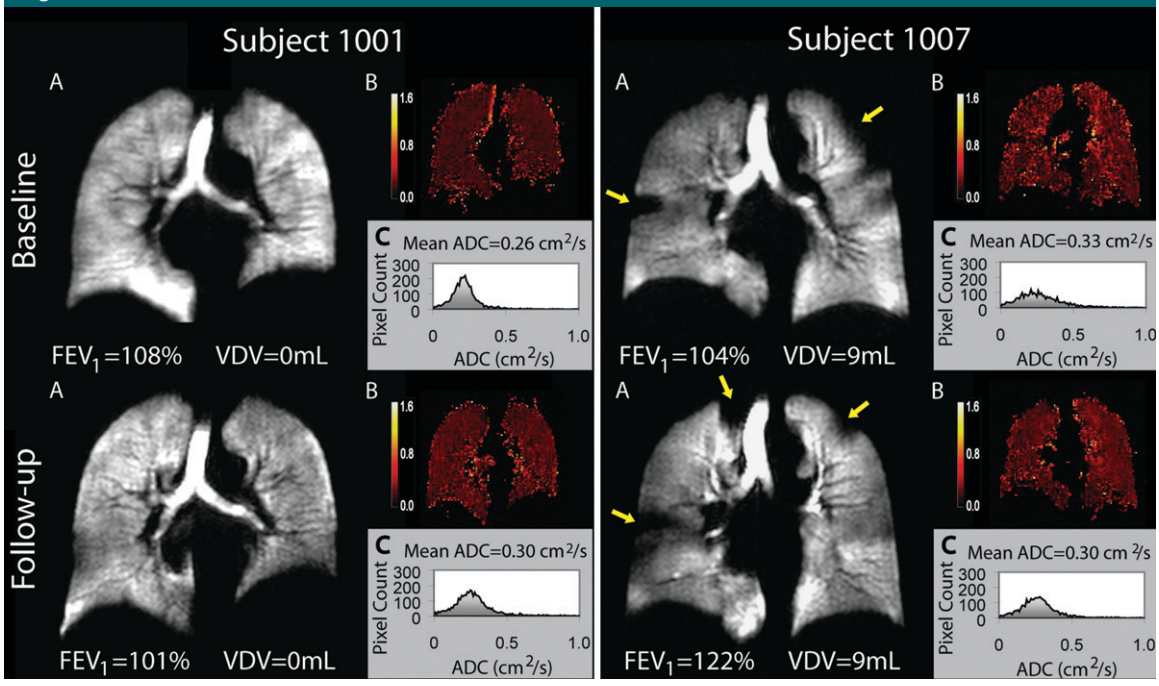

Figure 1: Representative hyperpolarized ^{3}He MR data at baseline (top) and follow-up (bottom) in healthy never-smokers. Left: *A,* Ventilation image, *B,* ADC map, and, *C,* ADC histogram in 58-year-old man (subject 1001). Right: *A,* Ventilation image, *B,* ADC map, and, *C,* ADC histogram in 73-year-old man (subject 1007).

Figure 2

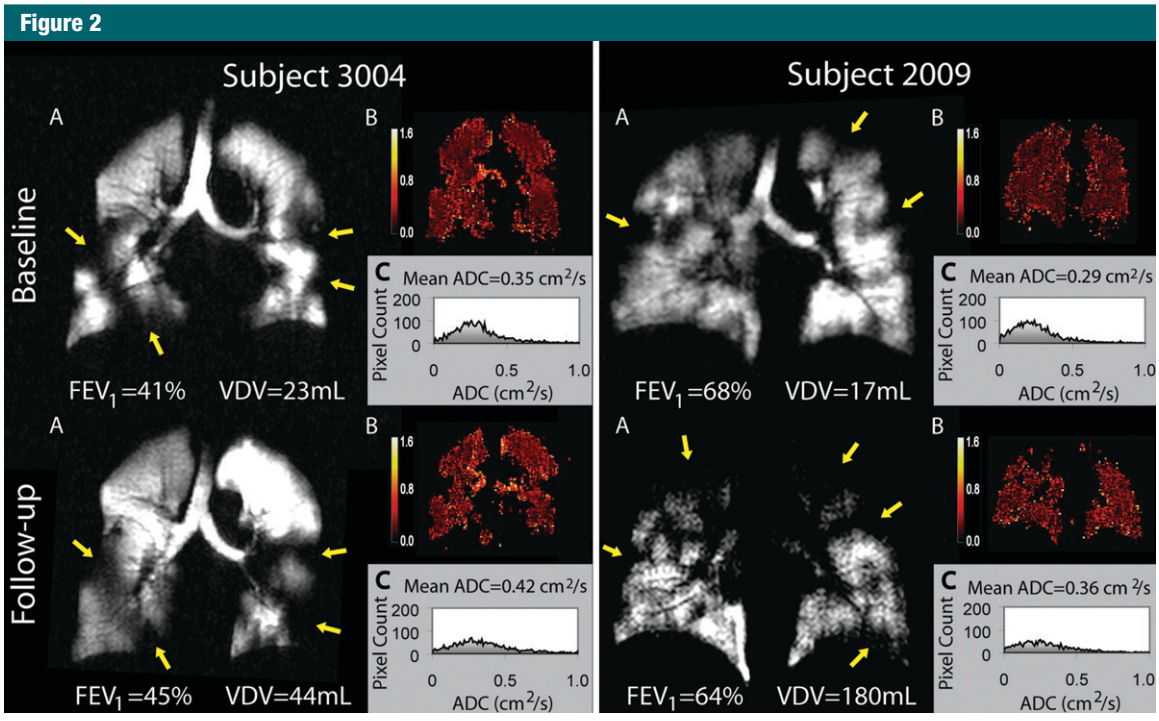

Figure 2: Representative hyperpolarized ^{3}He MR data show VDV and ADC changes during follow-up in COPD. Left: *A,* Ventilation image, *B,* ADC map, and, *C,* and ADC histogram in 75-year-old man with stage III COPD (subject 3004). Right: *A,* Ventilation image, *B,* ADC map, and, *C,* ADC histogram in 61-year-old man with stage II COPD (subject 2009). Top = baseline, bottom = follow-up.

Table 4

Relationship between FEV_1 Changes and ^{3}He MR Imaging Measurement Changes for Subjects with COPD over the Course of Time

Parameter	FEV_1 (L)	FEV_1 (Percentage Predicted)
Whole-lung ADC (cm^2/sec)	−0.02 (.93) [.93]	0.17 (.56) [>.99]
Center-section ADC (cm^2/sec)	−0.06 (.84) [>.99]	0.15 (.60) [.60]
Whole-lung VDV (L)	−0.56 (.03) [.09]	−0.53 (.04) [.12]
Center-section VDV (L)	−0.70 (.003) [.02]	−0.67 (.007) [.04]
Whole-lung VDP (%)	−0.60 (.02) [.08]	−0.55 (.03) [.12]
Center-section VDP (%)	−0.70 (.005) [.03]	−0.70 (.005) [.03]

Note.—Data are Spearman correlation coefficients, with *P* values in parentheses and Holm-Bonferroni–adjusted *P* values in brackets.

Figure 3

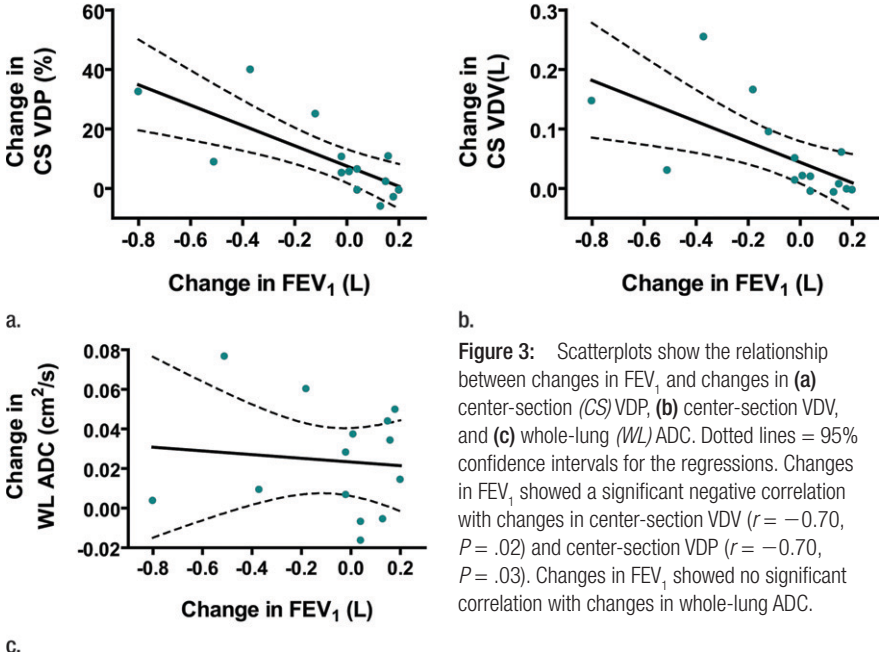

Figure 3: Scatterplots show the relationship between changes in FEV_1 and changes in **(a)** center-section *(CS)* VDP, **(b)** center-section VDV, and **(c)** whole-lung *(WL)* ADC. Dotted lines = 95% confidence intervals for the regressions. Changes in FEV_1 showed a significant negative correlation with changes in center-section VDV ($r = -0.70$, $P = .02$) and center-section VDP ($r = -0.70$, $P = .03$). Changes in FEV_1 showed no significant correlation with changes in whole-lung ADC.

Fletcher and Peto (3), as well as the more recent findings of a tiotropium intervention trial (43), we were not surprised to find that in ex-smokers with COPD, FEV_1 did not significantly change. Indeed, this study was not powered to detect such changes in FEV_1 during an approximately 2-year time frame; a retrospective power analysis showed that a sample size of approximately 1000 patients with COPD and 1000 healthy volunteers would be required to detect significant change in FEV_1 in this study. Unlike the Fletcher curve prediction that longitudinal changes in hyperpolarized ^{3}He MR imaging measurements in ex-smokers with COPD would be similar to those observed in healthy never-smokers, we observed an annualized rate of change in ^{3}He MR imaging–derived ADC of 0.01 cm^2/sec—an order of magnitude greater than the rate previously reported (0.001 cm^2/sec) for healthy nonsmokers in a cross-sectional multicenter study at 1.5 T (29) and for the healthy never-smokers reported in this study (0.002 cm^2/sec). In addition, we observed no significant change in ^{3}He MR imaging–derived ADC, ventilation defect measurements, or pulmonary function measurements for healthy never-smokers at follow-up. These preliminary longitudinal findings suggest that regional disease markers derived at noninvasive imaging can be used in a small number of subjects with COPD during short time periods to quantitatively detect significant changes.

We also showed that the change in ^{3}He MR imaging–derived VDV and VDP indicated a significant inverse correlation with the change in FEV_1, whereas the change in ADC showed no such relationship. This result suggests that ^{3}He MR imaging–derived ventilation defect measurements may be more predictive of airflow limitation than ^{3}He MR imaging–derived ADC, which necessitates further testing of this hypothesis. Although we observed statistically significant improvements in FEV_1 of less than 20 mL in five subjects with COPD, we did not observe a corresponding improvement in ^{3}He MR imaging–derived measurements during this time period. On the contrary, for these five subjects, we observed a statistically significant increase in ^{3}He MR imaging–derived ADC ($P = .02$) and no change in ventilation measurements. We believe this discordant finding highlights the sensitivity of using both ventilation and ADC measurements in detecting disease changes in COPD. In a related finding, Ohara and colleagues (15) showed a significant inverse correlation between annual changes in FEV_1 and CT measurement of wall area percentage (a surrogate of airway wall thickness), and, similar to our results, there was no significant relationship between the change in FEV_1 and emphysema (percentage of low attenuation areas). For five of 15 subjects with COPD evaluated in this pilot analysis, both imaging and spirometry results suggested disease progression. This finding generates a number of hypotheses to test in larger or longer imaging studies of COPD progression that will evaluate the relationship between exacerbations, treatment changes, and changes in quality of life with imaging and pulmonary function measurements. Future COPD studies that include hyperpolarized ^{3}He MR imaging will likely focus on a critical balance between longitudinal time frame

Figure 4

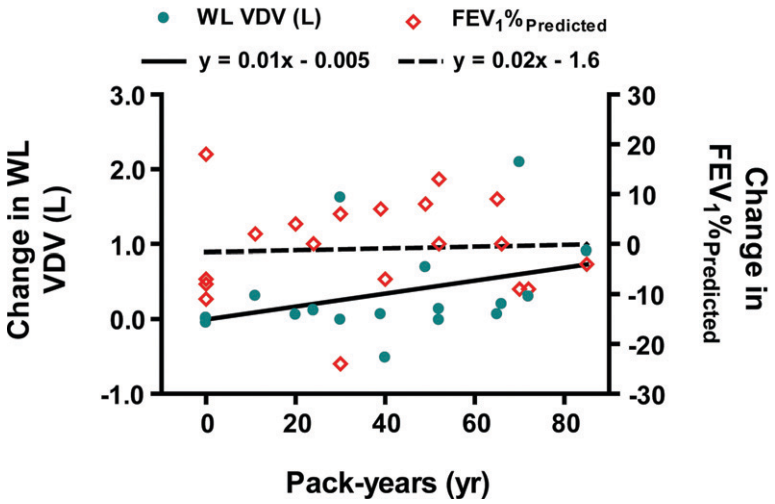

Figure 4: Scatterplot shows the relationship between smoking history and change in whole-lung *(WL)* VDV ($r = 0.52$; $P = .02$; $P = .06$, Holm-Bonferroni corrected) and change in FEV_1 (percentage predicted) ($r = 0.05$, $P = .83$).

and finite numbers of subjects because of the relative complexity of these studies and the prediction for increased costs and decreased availability of ^{3}He gas for clinical research (44). Nevertheless, the preliminary findings of this pilot hyperpolarized ^{3}He MR imaging longitudinal study provide clear guidance for future COPD imaging studies on established and emerging imaging tools such as optical coherence tomography (45), oxygen-enhanced and proton MR imaging methods (46,47), and hyperpolarized xenon 129 MR imaging.

Finally, we showed in an exploratory analysis, the potential relationship between smoking history and changes in ^{3}He MR imaging–derived VDV but not with changes in FEV_1. Previous cross-sectional studies suggest ongoing inflammation in ex-smokers with COPD (3,29) and that smoking history correlated with current inflammatory markers such as eosinophils (48) and vascular endothelial growth factor (49), which supports the hypothesis that there is a predictive relationship between pack-years and inflammation after smoking cessation. The results of this exploratory analysis of ^{3}He MR imaging changes and smoking history generate important hypotheses that future studies should explore in more detail.

Although this pilot study showed significant increases in ^{3}He MR imaging–derived measurements in just more than 2 years, we must acknowledge a number of specific limitations of our approach. We recognize that the relatively small group of subjects with COPD and healthy never-smokers who were evaluated and the relatively short period of follow-up compared with other COPD longitudinal studies (5) certainly limited the applicability of our results. The small sample size necessitates cautious interpretation of the results, as well as the future requirement for larger studies to test the hypotheses generated. For example, because of the small number of healthy volunteers and subjects with COPD evaluated, significant differences were not detected for pulmonary function measurements in either group. In addition, although we have previously demonstrated that ventilation defects are highly reproducible (20), the lack of longitudinal information regarding the variability of ventilation defects necessitates that the findings of this study be interpreted with caution.

Although this pilot study showed that ex-smokers with COPD differed from never-smokers, it was not designed to show the relationship between the significant imaging changes and more-established clinical measurements of COPD worsening. To make the important conclusion that ^{3}He MR imaging measurements are specifically related to clinical measurements of COPD worsening, future work in longer or larger studies must show that the detected ^{3}He MR imaging changes occurred in patients who had measureable clinical changes. Nevertheless, the results suggest that ^{3}He MR imaging provides a sensitive method for the detection of structural and functional changes of the lung that accompany COPD longitudinally. In the future, larger studies that directly compare ^{3}He MR imaging and other well-established clinical measurements of COPD progression will be required to better understand the relationship between ^{3}He MR imaging–derived measurements and other changes that occur in COPD over the course of time. In addition, a comparison of ex-smokers with COPD, healthy smokers, and current smokers with COPD may help to establish and directly compare rates of structural and functional decline of the lung. It will also be critical to track patient exacerbations and changes in treatment during longer time periods to probe potential treatment effects with imaging. We also acknowledge that for this pilot study, we limited the COPD cohort to those with minimal FEV_1 reversibility, although clearly many subjects with COPD have varying degrees of FEV_1 reversibility, which necessitates further work in such patients.

CT images were not prospectively acquired for this study; and therefore, our results cannot be directly compared with more-established CT measurements such as percentage of low attenuation areas (measurement of the extent of emphysema) or wall area percentage (measurement of airway wall thickness). Clearly, a direct comparison of CT and hyperpolarized ^{3}He MR imaging–derived measurements in the same subjects will allow for a better understanding of differences in measurement sensitivity these imaging modalities provide.

A previous study (32) has shown significant correlation between ADC and the measurement of diffusing capacity

of lung for carbon monoxide. A direct comparison in this study would have provided another quantitative measure of global emphysematous changes in these subjects. While Woods and colleagues (28) have previously shown the significant correlation between ^{3}He MR imaging–derived ADC and histologic measurements of emphysema, we have not yet determined the underlying disease that results in the ^{3}He MR imaging–derived ventilation defects we observe, which may be a result of small airway occlusion, mucous plugs, airway wall thickening and inflammation, or bullous disease. Related to this is the fact that there is important information in regions of intermediate signal intensity and in both hyper- and hypointense regions that has not yet been quantitatively or spatially exploited. The development and validation of ^{3}He MR image analysis techniques that quantify heterogeneous signal intensity information are required in the future to fully characterize the important ventilation information contained on the image. Whether regions of diminished ventilation and emphysema develop independently and the extent to which one leads to the other cannot be ascertained by results of this preliminary longitudinal study and has yet to be determined in other longitudinal imaging studies. Importantly, however, our group previously described the high reproducibility of ^{3}He MR imaging–derived ventilation defects in COPD (20), suggesting that the significant changes measured in this study may be because of changes in lung morphology or function and not because of the variability of the imaging or measurement technique or because of short-term changes in small airway diameter or patency.

In summary, in this small pilot study of ex-smokers with COPD, by using ^{3}He MR imaging we detected significant lung changes that occurred during a relatively short time period, perhaps before FEV_1 changes could be detected or perhaps because such longitudinal changes occurred within the FEV_1 silent zones, where disease might have accumulated without detection.

Acknowledgments: We thank Shayna McKay, BSc, and Sandra Halko, CCRC, RPT, for clinical coordination and clinical database management, Adam Farag, MSc, for production and dispensing of ^{3}He gas, and Cynthia Harper-Little, RMT, for MR imaging of research volunteers. The use of an on-site hyperpolarized ^{3}He gas polarizer (HeliSpin; GE Healthcare, Durham, NC) was provided to Robarts Research Institute through an agreement between GE Healthcare and Merck (2005–2008) and between Robarts Research Institute and GE Healthcare (2008–onward).

References

1. Mannino DM, Buist AS. Global burden of COPD: risk factors, prevalence, and future trends. Lancet 2007;370(9589):765–773.
2. World Health Organization. Global surveillance, prevention and control of chronic respiratory diseases: a comprehensive approach. Geneva, Switzerland: World Health Organization, 2007.
3. Fletcher C, Peto R. The natural history of chronic airflow obstruction. BMJ 1977;1(6077):1645–1648.
4. Rabe KF, Hurd S, Anzueto A, et al. Global strategy for the diagnosis, management, and prevention of chronic obstructive pulmonary disease: GOLD executive summary. Am J Respir Crit Care Med 2007;176(6):532–555.
5. Vestbo J, Anderson W, Coxson HO, et al. Evaluation of COPD Longitudinally to Identify Predictive Surrogate Endpoints (ECLIPSE). Eur Respir J 2008;31(4):869–873.
6. Burrows B, Fletcher C, Heard BE, Jones NL, Wootliff JS. The emphysematous and bronchial types of chronic airways obstruction: a clinicopathological study of patients in London and Chicago. Lancet 1966;1(7442):830–835.
7. Pistolesi M, Camiciottoli G, Paoletti M, et al. Identification of a predominant COPD phenotype in clinical practice. Respir Med 2008;102(3):367–376.
8. Hayhurst MD, MacNee W, Flenley DC. Diagnosis of pulmonary emphysema by computerised tomography. Lancet 1984;2(8398):320–322.
9. Müller NL, Staples CA, Miller RR, Abboud RT. "Density mask": an objective method to quantitate emphysema using computed tomography. Chest 1988;94(4):782–787.
10. Gevenois PA, de Maertelaer V, De Vuyst P, Zanen J, Yernault JC. Comparison of computed density and macroscopic morphometry in pulmonary emphysema. Am J Respir Crit Care Med 1995;152(2):653–657.
11. Coxson HO, Rogers RM, Whittall KP, et al. A quantification of the lung surface area in emphysema using computed tomography. Am J Respir Crit Care Med 1999;159(3):851–856.
12. Nakano Y, Wong JC, de Jong PA, et al. The prediction of small airway dimensions using computed tomography. Am J Respir Crit Care Med 2005;171(2):142–146.
13. Nakano Y, Müller NL, King GG, et al. Quantitative assessment of airway remodeling using high-resolution CT. Chest 2002;122(6 suppl):271S–275S.
14. Nakano Y, Muro S, Sakai H, et al. Computed tomographic measurements of airway dimensions and emphysema in smokers: correlation with lung function. Am J Respir Crit Care Med 2000;162(3 pt 1):1102–1108.
15. Ohara T, Hirai T, Sato S, et al. Longitudinal study of airway dimensions in chronic obstructive pulmonary disease using computed tomography. Respirology 2008;13(3):372–378.
16. de Lange EE, Mugler JP 3rd, Brookeman JR, et al. Lung air spaces: MR imaging evaluation with hyperpolarized ^{3}He gas. Radiology 1999;210(3):851–857.
17. Kauczor HU, Ebert M, Kreitner KF, et al. Imaging of the lungs using 3He MRI: preliminary clinical experience in 18 patients with and without lung disease. J Magn Reson Imaging 1997;7(3):538–543.
18. Möller HE, Chen XJ, Saam B, et al. MRI of the lungs using hyperpolarized noble gases. Magn Reson Med 2002;47(6):1029–1051.
19. Salerno M, Altes TA, Brookeman JR, de Lange EE, Mugler JP 3rd. Dynamic spiral MRI of pulmonary gas flow using hyperpolarized (3)He: preliminary studies in healthy and diseased lungs. Magn Reson Med 2001;46(4):667–677.
20. Mathew L, Evans A, Ouriadov A, et al. Hyperpolarized 3He magnetic resonance imaging of chronic obstructive pulmonary disease: reproducibility at 3.0 tesla. Acad Radiol 2008;15(10):1298–1311.
21. Yablonskiy DA, Sukstanskii AL, Leawoods JC, et al. Quantitative in vivo assessment of lung microstructure at the alveolar level with hyperpolarized 3He diffusion MRI. Proc Natl Acad Sci U S A 2002;99(5):3111–3116.
22. Salerno M, Altes TA, Mugler JP 3rd, Nakatsu M, Hatabu H, de Lange EE. Hyperpolarized noble gas MR imaging of the lung: potential clinical applications. Eur J Radiol 2001;40(1):33–44.
23. Saam BT, Yablonskiy DA, Kodibagkar VD, et al. MR imaging of diffusion of (3)He gas

in healthy and diseased lungs. Magn Reson Med 2000;44(2):174–179.

24. Salerno M, de Lange EE, Altes TA, Truwit JD, Brookeman JR, Mugler JP 3rd. Emphysema: hyperpolarized helium 3 diffusion MR imaging of the lungs compared with spirometric indexes—initial experience. Radiology 2002;222(1):252–260.
25. Kauczor HU, Hofmann D, Kreitner KF, et al. Normal and abnormal pulmonary ventilation: visualization at hyperpolarized He-3 MR imaging. Radiology 1996;201(2):564–568.
26. MacFall JR, Charles HC, Black RD, et al. Human lung air spaces: potential for MR imaging with hyperpolarized He-3. Radiology 1996;200(2):553–558.
27. Ley S, Zaporozhan J, Morbach A, et al. Functional evaluation of emphysema using diffusion-weighted 3Helium-magnetic resonance imaging, high-resolution computed tomography, and lung function tests. Invest Radiol 2004;39(7):427–434.
28. Woods JC, Choong CK, Yablonskiy DA, et al. Hyperpolarized 3He diffusion MRI and histology in pulmonary emphysema. Magn Reson Med 2006;56(6):1293–1300.
29. Fain SB, Altes TA, Panth SR, et al. Detection of age-dependent changes in healthy adult lungs with diffusion-weighted 3He MRI. Acad Radiol 2005;12(11):1385–1393.
30. Evans A, McCormack D, Ouriadov A, Etemad-Rezai R, Santyr G, Parraga G. Anatomical distribution of 3He apparent diffusion coefficients in severe chronic obstructive pulmonary disease. J Magn Reson Imaging 2007;26(6):1537–1547.
31. Evans A, McCormack DG, Santyr G, Parraga G. Mapping and quantifying hyperpolarized 3He magnetic resonance imaging apparent diffusion coefficient gradients. J Appl Physiol 2008;105(2):693–699.
32. Fain SB, Panth SR, Evans MD, et al. Early emphysematous changes in asymptomatic smokers: detection with 3He MR imaging. Radiology 2006;239(3):875–883.
33. Parraga G, Ouriadov A, Evans A, et al. Hyperpolarized 3He ventilation defects and apparent diffusion coefficients in chronic obstructive pulmonary disease: preliminary results at 3.0 Tesla. Invest Radiol 2007;42(6):384–391.
34. Swift AJ, Wild JM, Fichele S, et al. Emphysematous changes and normal variation in smokers and COPD patients using diffusion 3He MRI. Eur J Radiol 2005;54(3):352–358.
35. Choudhri A, Altes TA, Stay R, Mugler JP 3rd, de Lange EE. The occurrence of ventilation defects in the lungs of healthy subjects as demonstrated by hyperpolarized helium-3 MR imaging [abstr]. In: Radiological Society of North America Scientific Assembly and Annual Meeting Program. Oak Brook, Ill: Radiological Society of North America, 2007; 280.
36. Rodriguez-Roisin R. Toward a consensus definition for COPD exacerbations. Chest 2000;117(5 suppl 2):398S–401S.
37. Pellegrino R, Viegi G, Brusasco V, et al. Interpretative strategies for lung function tests. Eur Respir J 2005;26(5):948–968.
38. Mathew L, McCall JM, McKay S, et al. Hyperpolarized 3He magnetic resonance imaging of ventilation defect volume variability in COPD [abstr]. In: Proceedings of the Fifteenth Meeting of the International Society for Magnetic Resonance in Medicine. Berkeley, Calif: International Society for Magnetic Resonance in Medicine, 2007; 276.
39. de Lange EE, Altes TA, Patrie JT, et al. The variability of regional airflow obstruction within the lungs of patients with asthma: assessment with hyperpolarized helium-3 magnetic resonance imaging. J Allergy Clin Immunol 2007;119(5):1072–1078.
40. Woodhouse N, Wild JM, Paley MN, et al. Combined helium-3/proton magnetic resonance imaging measurement of ventilated lung volumes in smokers compared to never-smokers. J Magn Reson Imaging 2005;21(4):365–369.
41. VanBell G, Fisher L, Heagerty P, Lumley T. Multiple comparisons. In: Biostatistics: a methodology for the health sciences. 2nd ed. Seattle, Wash: Wiley-Interscience, 2004.
42. Howell DC. Fundamental statistics for the behavioral sciences. Belmont, Calif: Brooks/Cole–Thomas Learning, 2004.
43. Tashkin DP, Celli B, Kesten S, Lystig T, Mehra S, Decramer M. Long-term efficacy of tiotropium in relation to smoking status in the UPLIFT trial. Eur Respir J 2010;35(2):287–294.
44. Schwarzschild B. Inhaling hyperpolarized noble gas helps magnetic resonance imaging of lungs. Phys Today 1995;48(6):17–18.
45. Coxson HO, Quiney B, Sin DD, et al. Airway wall thickness assessed using computed tomography and optical coherence tomography. Am J Respir Crit Care Med 2008;177(11):1201–1206.
46. Ohno Y, Koyama H, Matsumoto K, et al. Oxygen-enhanced MRI vs. quantitatively assessed thin-section CT: pulmonary functional loss assessment and clinical stage classification of asthmatics. Eur J Radiol 2009 Jul 29. [Epub ahead of print]
47. Ohno Y, Iwasawa T, Seo JB, et al. Oxygen-enhanced magnetic resonance imaging versus computed tomography: multicenter study for clinical stage classification of smoking-related chronic obstructive pulmonary disease. Am J Respir Crit Care Med 2008;177(10):1095–1102.
48. Dippolito R, Foresi A, Chetta A, et al. Eosinophils in induced sputum from asymptomatic smokers with normal lung function. Respir Med 2001;95(12):969–974.
49. Rovina N, Papapetropoulos A, Kollintza A, et al. Vascular endothelial growth factor: an angiogenic factor reflecting airway inflammation in healthy smokers and in patients with bronchitis type of chronic obstructive pulmonary disease? Respir Res 2007;8:53.